AFRL-AFOSR-CL-TR-2020-0001

Multi-lateral defense science partnering to investigate fundamental bio-electrical-chemical interaction mechanism of aerospace materials

Nelson Vejar
ACADEMIA POLITECNICA AERONAUTICA
Gran Av. Jose Miguel Carrera
Santiago, CP/8020744
CL

07/17/2020
Final Report

Air Force Research Laboratory
Air Force Office of Scientific Research
Southern Office of Aerospace Research and Development
U.S. Embassy Santiago, AV. Andrews Bello 2800 Santiago, Chile

REPORT DOCUMENTATION PAGE

Form Approved
OMB No. 0704-0188

1. REPORT DATE *(DD-MM-YYYY)*	2. REPORT TYPE	3. DATES COVERED *(From - To)*
17-07-2020	Final	15 Dec 2018 to 14 Dec 2019

4. TITLE AND SUBTITLE
Multi-lateral defense science partnering to investigate fundamental bio-electrical-chemical interaction mechanism of aerospace materials

5a. CONTRACT NUMBER

5b. GRANT NUMBER
FA9550-19-1-0061

5c. PROGRAM ELEMENT NUMBER
61102F

6. AUTHOR(S)
Nelson Vejar

5d. PROJECT NUMBER

5e. TASK NUMBER

5f. WORK UNIT NUMBER

7. PERFORMING ORGANIZATION NAME(S) AND ADDRESS(ES)
ACADEMIA POLITECNICA AERONAUTICA
Gran Av. Jose Miguel Carrera
Santiago, CP/8020744 CL

8. PERFORMING ORGANIZATION REPORT NUMBER

9. SPONSORING/MONITORING AGENCY NAME(S) AND ADDRESS(ES)
AFOSR/SOARD
U.S. Embassy Santiago
Av. Andres Bello 2800
Santiago, Chile

10. SPONSOR/MONITOR'S ACRONYM(S)
AFRL/AFOSR IOS

11. SPONSOR/MONITOR'S REPORT NUMBER(S)
AFRL-AFOSR-CL-TR-2020-0001

12. DISTRIBUTION/AVAILABILITY STATEMENT
A DISTRIBUTION UNLIMITED: PB Public Release

13. SUPPLEMENTARY NOTES

14. ABSTRACT
Microbiologically influenced corrosion (MIC) have been widely studied because the phenomenon can promote the localized degradation of metallic materials exposed to many different environments. The present work is a study focused on the electrochemical behavior of Aluminium alloy (AA) 2024-T3 exposed to a sterile and inoculated simulated saline medium. The bacteria were collected from corrosion products of Thailand aircraft. The 16S ribosomal RNA sequence results show a closely related to Bacillus genus (Gram positive), as Bacillus safensis (~99.68 %), and Bacillus pumilus (~99.73 %). The influence of different bacteria attached on the AA2024-T3 surface was evaluated using electrochemical techniques, such as linear sweet voltammetry and impedance spectroscopy at open circuit and cathodic overpotential. Electrochemical results suggest (a) a change of the double layer capacitance in presence of bacteria, and (b) a substantial disparity in the electrochemical response in the cathodic reaction of AA2024-T3 influenced by microorganisms, indicating that the inoculated media promote the catalysis of a redox half-reaction of oxygen reduction to water.

15. SUBJECT TERMS
bio-corrosion, microbially-induced corrosion

16. SECURITY CLASSIFICATION OF:			17. LIMITATION OF ABSTRACT	18. NUMBER OF PAGES	19a. NAME OF RESPONSIBLE PERSON
a. REPORT	b. ABSTRACT	c. THIS PAGE			ANDERSEN, GEOFFREY
Unclassified	Unclassified	Unclassified	SAR		19b. TELEPHONE NUMBER *(Include area code)* 703-615-9465

Standard Form 298 (Rev. 8/98)
Prescribed by ANSI Std. Z39.18

FINAL REPORT

Multi-Lateral Defense Science Partnering to Investigate Fundamental Bio-Electro-Chemical Interaction Mechanism of Aerospace Materials

FA9550-19-1-0061

Abstract

Microbiologically influenced corrosion (MIC) have been widely studied because the phenomenon can promote the localized degradation of metallic materials exposed to many different environments. The present work is a study focused on the electrochemical behavior of Aluminium alloy (AA) 2024-T3 exposed to a sterile and inoculated simulated saline medium. The bacteria were collected from corrosion products of Thailand aircraft. The 16S ribosomal RNA sequence results show a closely related to *Bacillus genus* (Gram positive), as *Bacillus safensis* (~99.68 %), and *Bacillus pumilus* (~99.73 %). The influence of different bacteria attached on the AA2024-T3 surface was evaluated using electrochemical techniques, such as linear sweet voltammetry and impedance spectroscopy at open circuit and cathodic overpotential. Electrochemical results suggest (a) a change of the double layer capacitance in presence of bacteria, and (b) a substantial disparity in the electrochemical response in the cathodic reaction of AA2024-T3 influenced by microorganisms, indicating that the inoculated media promote the catalysis of a redox half-reaction of oxygen reduction to water.

1 INTRODUCTION

In the aircraft industry, the AA2024-T3 is an important material extensively used to build structures and as brittle sections of the airplanes. The most common deterioration process influenced by salinity is the localized corrosion, which is related to the dealloying of the second faces, particularly copper rich of Al_2CuMg [1],[2]. Moreover, the presence of the alloying elements in these materials makes them susceptible to bacterial attachment. A great number of reports on aircraft deterioration are related to microbial growth by contamination inside fuel storage tanks and aircraft wing tanks, this phenomenon is known as microbiologically influenced corrosion (MIC) [3],[4],[5]. As expected, corrosion and biocorrosion increase maintenance costs and time of the aircraft in the hangar. Therefore, the growing interest is to shed light on these issues and develop future inhibition methods.

The importance of the evaluation of microorganism's activities on the metal surface is based on two parallel processes, (a) bacteria development in formation and growth of biofilm, and (b) metal deterioration (corrosion), both phenomena involve some electrochemical mechanisms. Although the electrochemical nature of aqueous corrosion is universally accepted, often the redox reactions sustained on cell membrane of bacteria or inner mitochondrial membrane are omitted in the environment process [6],[7]. Bacteria catalyze, during the step of growth and development, imperceptibly slow electrochemical cell reactions for metabolism [8],[9]. The metabolic products (or waste), produced by bacteria and excreted to surrounding media, might be corrosive or might degrade protective surface-oxide passive films of aluminium alloy [10]. The rates of microbial reactions are limited by environmental factors such as substrate and nutrient availability, but they are still fast enough to develop a MIC in conditions where little or no corrosion is normally expected [11]. The MIC related to AA2024-T3 has been evaluated under several conditions, however, in a tropical environment, specifically the one of Thailand region, the information is poor [3].

The electrochemical techniques to evaluate de corrosion behavior, in simulated conditions, has been an important analysis method. At present, electrochemical impedance spectroscopy (EIS), is a key to understand the degradation of metallic materials by (a) analyzing of the oxide film dissolution [10], and (b) evaluating the contribution of each redox half-reaction using cathodic and anodic polarization [12]. In this study, EIS at open circuit potential (E_{OC}) was used to the evaluation of oxide film dissolution, and cathodic polarization to evaluate the influence of bacteria on the oxygen reduction in the corrosion process of AA2024-T3.

The Bacillus genus bacteria related MIC with AA 2024-T3 has been previously reported by Rajasekar et al. who reported an aggressive, facultative anaerobes and hydrocarbon-degrading bacteria, Bacillus cereus [24], the microbial capacity associated with alloy degradation was related to enzymatic activity. Deen *et al*. studied, under aerobic condition, the electrochemical behavior of Al-Cu alloy exposed to Bacillus megaterium bacteria [25]. The morphology and growth pattern of localized dissolution of aluminium suggested the corrosion mechanism as microbial assisted pitting. On the other hand, the presence of bacteria influences the passivity of alloy, Ortega et al. evaluated the microbiological influence of Bacillus toyonensis on the resistivity of polarization of anodized AA2024 [26]. They found that this bacteria promote the passivation of oxide film related to the influence of the bacteria activity with the dissolution/formation of oxide film equilibria. Both effects of corrosive and protective behavior of different bacteria are widely discussed by scientists in order to understand the limit line of these processes [27].

Objective Evaluate In this work, two bacteria were collected and isolated (B1-19 and B2-14) from the undercarriage of an aircraft. Using 16S rDNA sequence analysis, the bacteria were closely related to *Bacillus safensis* strain NBRC 1000820 (B1-19, ~99.68%), and *Bacillus pumilus* strain NBRC 12092 (B2-14, ~99.73%). The aircraft under study is operative in a tropical region, Thailand, thus, the experiments were carried out in simulated tropical conditions in temperature term, additionally the influence of coast environment were considered by adding to the solution NaCl 0.1 M.

2 EXPERIMENTAL

2.1. Specimen pre-treatment

The metallic samples consisted of AA2024-T3, provided by the Empresa Nacional de Aeronáutica de Chile (ENAER). The chemical composition of this alloy was: 0.078 Si, 0.153 Fe, 5.240 Cu, 0.770 Mn, 1.380 Mg, 0.008 Cr, 0.007 Ni, 0.023 Zn, 0.036 Ti, 0.013 Sn, 0.004 Bi, balance Al (wt. %). The specimens consisted of 50 X 50 X 0.2 mm plates machined from a rolled plate. The surface of each sample was polished mechanically using # 800, and 1200 SiC paper, then, the samples were washed using ethanol and an ultrasonic device for 5 minutes. Finally, the surfaces were exposed for 12 minutes to UV light in a laminar flow chamber to be sterilized [13].

2.2. Isolation and identification of bacteria strains from corrosion products

The bacterial strains were obtained from corrosion products of the undercarriage of an aircraft exposed to the tropical environment of Thailand. The corrosion product was placed in sterile plastic receptacles and transported in a cooler packed to the laboratory. Then, corrosion products were added aseptically to sterile nutritive broth (Luria Bertani, LB) for bacterial growth. The LB media consisted of 10 g tryptone, 5 g yeast extract, and 10 g NaCl per Liter of water (ultra purus, Mili Q quality, 18.2 $M\Omega \cdot cm^{-1}$). Cultured bacteria were isolated through successive serial dilutions and conventional plating from the general enrichment conditions [14]. Two isolated strains were obtained (B1-19 and B2-14) and stored at -18 °C to ensure the purity and consistency of the bacterial material in all subsequent experiments.

The microorganisms were identified on 16s rRNA gene sequencing (Centro de Genómica y Bioinformática, Universidad Mayor). Sequences obtained were assembled, analyzed, and manually edited using ChromasPro software (Technelysium Pty Ltd.) for a final sequence extension of (~450 bp). Strains were taxonomically classified using the Naïve Bayesian rRNA Classifier function from the RDP-Ribosome Database Project [15]. To determine the phylogenetic distance between the bacteria isolated and other bacterial strains with 16s rRNA gene sequences available on databases, a neighbor joining tree based on 16S rRNA gene sequences was generated using the NCBI Blast database. A 97-100% match of the genetic material unknown with the GenBank data set was considered as an acceptable identification [16].

2.3 Culture media preparation

Sterilized plates of AA2024-T3 were exposed to sterile simulated medium (SSM) as control, which was composed by 2.3 mM of $(NH_4)_2SO_4$, 8.8 mM of KH_2PO_4, 1 mM of $MgSO_4$ X 7 H_2O, 1.7 mM of $CaCl_2$ X $2H_2O$, 0.024 g/L of yeast extract, 0.024 g/L of Tryptone, plus 0.1 M of NaCl [13]. For the experiments inoculated with bacteria, the same electrolyte was used. The inoculation of microorganisms was performed using 10% v/v of the bacteria in SSM, previously grown in LB medium at 30 °C over-night, and pelleted. The culture was inoculated to 10^8 CFU/mL. To maintain bacterial density near to the steady state growth phase during the experiment, every 4 days 70 % of the medium was eliminated and replaced with fresh SSM, and the bacteria were re-inoculated. The experiments were performed in an electrochemical cell used previously [10], and kept at 30 °C and which may have undergone fluctuations by ± 2 °C. Each system was performed in triplicate to guaranty reproducibility.

2.4 Microbiologically influenced corrosion test

Electrochemical measurements were performed with a three-electrode configuration. The working electrode was a plate electrode of AA2024-T3 placed at the bottom of the electrochemical cell, with a surface area of 16.61 cm^2. A pure graphite rod (diameter, 6 mm) and a saturated calomel electrode (SCE) were used as a counter electrode and reference electrode, respectively.

The electrochemical measurements were carried out using a VSP potentiostat (Bio-Logic, USA) for 1, 8 and 12 days of exposure to sterile and inoculated SSM medium at 30°C ± 2 °C. The open circuit potential (E_{OC}) was measured until its stabilization (± 10 mV) prior to each Electrochemical Impedance Spectroscopy (EIS) and Linear Sweep Voltammetry (LSV) tests. LSV test was performed in cathodic and anodic overpotential by separately at $E_{cathodic} = E_{OC}$ - 145 mV and $E_{anodic} = E_{OC}$ + 250 mV respectively, at a sweep rate of 0.1 $mV{\cdot}s^{-1}$ [17]. The EIS was carried out at OCP potential and at $E=E_{OC}$-50 mV in a frequency range of 10 mHz – 10 kHz with 7 points per decade and 10 mV peak to peak sinusoidal voltage. The impedance results were fitted by using a home-developed software called SIMAD (LISE UPR 15 CNRS, France), adjustment every 1200 iterations until reaching the lowest $\chi 2$ value.

2.5 Morphological characterization

After 12 days of exposition in sterile and inoculated medium with bacteria, the metallic surfaces of AA2024-T3 were examined using a scanning electron microscope (JEOL, model JSM-6010LA) coupled with an energy dispersive X-ray spectrometer (EDS), to characterize the morphology and elemental composition of the oxide film. SEM observation was carried out with beam voltage of 14-15 kV. The metallic samples were cleaned to removing the biofilm using an ultrasonic ethanolic bath (Elma, model S3H) for 5 minutes.

The bacteria under study were observed by an optical microscope (Bio2T-PLLedpplan, BEL ENGINEERING) in order to characterize their morphology, shape, and size.

3 RESULTS AND DISCUSSION

3.1 Bacteria identification

Two bacteria were isolated (B1-19 and B2-14) through several serial dilutions and plating rounds in LB media. The 16S rDNA sequence analysis was used to identify. The results showed a close affiliation to *Bacillus safensis* strain (B1-19, ~99.68%), and *Bacillus pumilus* strain (B2-14, ~99.73%) using BLAST search database [18]. Figure 1 shows the neighbor joining tree based on 16S rRNA gene sequences, revealing phylogenetic relationships.

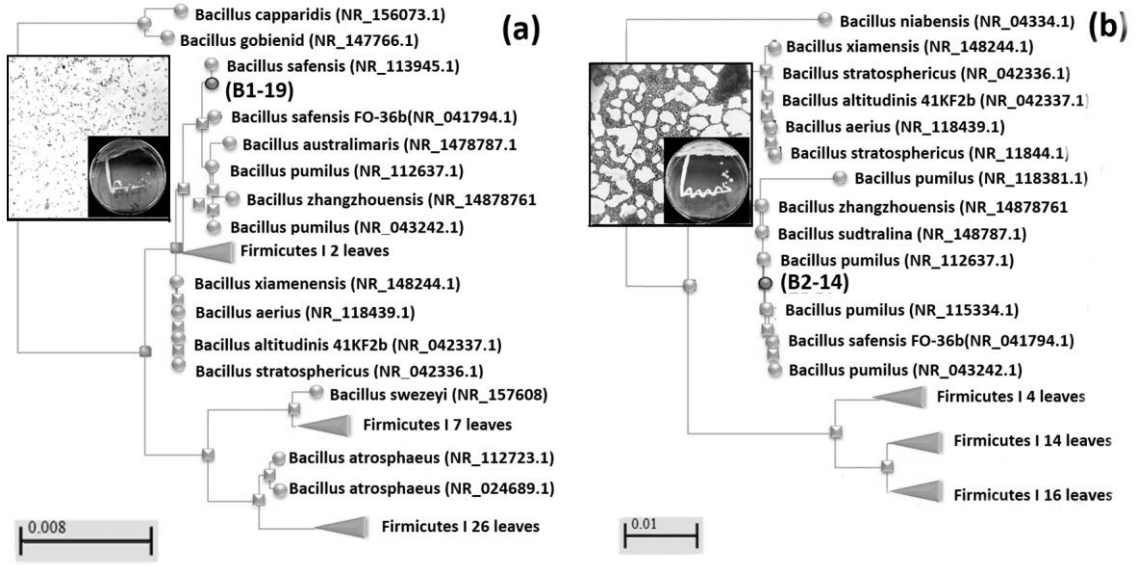

Figure 1. Phylogenetic tree of members of the genus Bacillus, based on 16S rRNA gene sequences of the highly corrosive bacterial isolate. The tree was constructed using the neighbor-joining method. To *Bacillus safensis* (a) and *Bacillus pumilus* (b) tree, the bars of genetic distance used were 0.008 and 0.01 respectively.

Bacillus safensis is a Gram-positive, mesophilic, spore-forming, aerobic and chemo-heterotrophic bacterium. It is a rod-shaped and motile bacterium coinciding with that found in the literature from bacterial identification [19]. Moreover, the *Bacillus safensis* was reported and found in spacecraft surfaces (Mars Odyssey Orbiter) and assembly-facility surfaces at the Jet Propulsion Laboratory in California and the Kennedy Space Center in Florida [20]. *Bacillus pumilus* is an important and second most dominant species among the aerobic spore-forming bacteria [21]. A considerable number of these *Bacillus pumilus* isolates have exhibited high resistance to reactive oxygen species as H_2O_2 [22], and are thus considered as "problematic" micro-organisms, since H_2O_2 is recommended for the bio-reduction of spacecraft component [23]. The relationship between this kind of bacteria and aluminium alloy has been not described yet.

3.2 Linear Sweep Voltammetry

The LSV results of AA2024-T3 exposed to the different conditions are shown in Figure 2. The electrochemical parameters and the values of current density at anodic and cathodic zone (i_a, i_c) have been estimated from LSV and are summarized in **¡Error! No se encuentra el origen de la referencia.**. The values of i_a, and i_c were estimated from Open Circuit potential (E_{OC}) values, E_{anodic}= (E_{OC} + 30 mV) and $E_{cathodic}$ = (E_{OC} - 30mV) respectively. The results show that the bacteria *B. safensis* and *B. pumilus* present a greater i_c at 1 day of exposure, in comparison to the sample exposed to the sterile medium. The effect of the increasing i_c could be attributed to the increasing rate of oxygen reduction reaction on the AA2024-T3 surface [12]. At the same time, the i_a of AA2024-T3 values decreasing in the presence of bacteria, in comparison with metallic samples exposure to the sterile medium.

After 8 days and 12 days of exposure, the i_c of AA2024-T3 decreasing in presence of bacteria *B. safensis* and *B. pumilus* compare with samples exposed to sterile media, likewise i_a increasing in presence of both bacteria, compared with samples exposed to sterile media (showed in supplementary material Figure S1). The low current density of AA2024-T3 exposed to bacteria could be related to a drop in the bacterial metabolic activity, and the development of protective biofilms [24]. As was observed the E_{OC} values of AA2024-T3 were shifted to cathodic direction from day 1 to day 8, and the magnitude of these displaced could be controlled by bacteria,

and could be related to the influence of bacteria on the cathodic reaction of oxygen reduction, a mechanism previously reported of MIC of AA2024-T3 in aerobic condition [25].

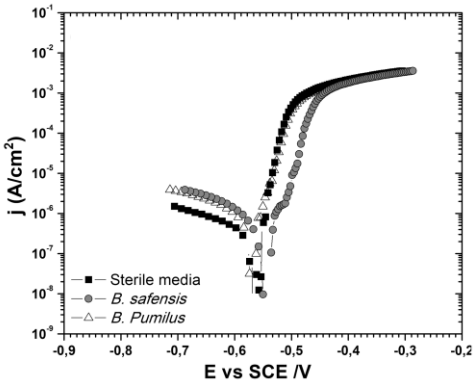

Figure 2 Linear sweep voltammetry (LSV) of AA2024-T3 after (a) 1 day, (b) 8 days, and (c) 12 days of exposure.

From a qualitative point of view, an analysis of Figure 2 about of passive zone was made, in order to understand the phenomenon of corrosion. The LSV plot shown clearly an unstable and brittle aluminium oxide film, which is verified as a break in the curve (or broke curve) in the zone near to corrosion potential with the absence of a plateau at the exposure time of 1 day for all systems. This behavior decreased with the time of exposition, at 8 days is possible to see a plateau followed by an increase of current density associated to a local corrosion, and the effect of poor quality of aluminium oxide film was most important of AA2024-T3 exposed to *B. safensis*. At 12 days, the plateau is larger than before days, and the presence of the pitting corrosion (E_{pit}) is observed. Moreover, the passivation potential ($E_{passivation}$= E_{oc}-E_{pit}) is influenced by bacteria, decreasing the $E_{passivation}$ approach to 100 mV from E_{OC} values, indicating a susceptibility to local corrosion of AA2024-T3 exposed to bacteria [26]. The summarized of parameters are shown in Table S1, in supplementary materials.

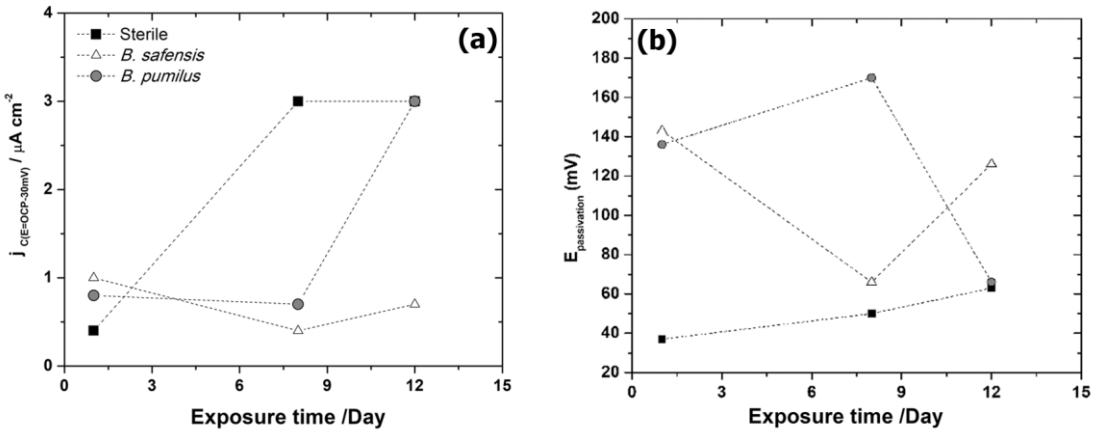

Figure 3 Parameters from LVS results (a) i_c and (b) Potential of passivation.

3.3 Electrochemical Impedance Spectroscopy at E_{OC}

Figure 4 shows the Nyquist plots of AA2024-T3 after being exposed to sterile and inoculated media with *B. safensis* and *B. pumilus* for 1, 8 and 12 days. The graphs reveal a decreasing of the total impedance as a function of exposition time, exhibiting the lowest value at 12 days, and a marked capacitive behavior to low-frequency (LF) range in all evaluated systems. At short exposure time, impedance response shows a similar behavior between sterile and inoculated media in the whole frequency range. However, the impedance

response of *B. safensis* and *B. pumilus* demonstrated to have an evolution across exposure time. For instance, *B safensis* decreased continually as a function of exposure time, while *B. pumilus* demonstrated a decrease after 8 days and remained constant until 12 days.

The capacitive loops of the aluminium alloy correspond to a constant phase element (CPE) behavior [27]. In sterile media after 1 day of exposure time, it possible to observe two time constants, one at High Frequency (HF) and other at LF as was observed by G. Boisier *et al.* on AA2024 [28]. This behavior was observed in almost all evaluated systems, showed in the supplementary material (Figure S2). The loops at HF and LF range are related to the oxide film and the double-layer capacitance (C_{dl}), respectively. In order to characterize both responses, the impedance parameters were obtained, including the complex capacitance (C_∞) at the HF [29]. Impedance parameters also were summarized in **¡Error! No se encuentra el origen de la referencia.**.

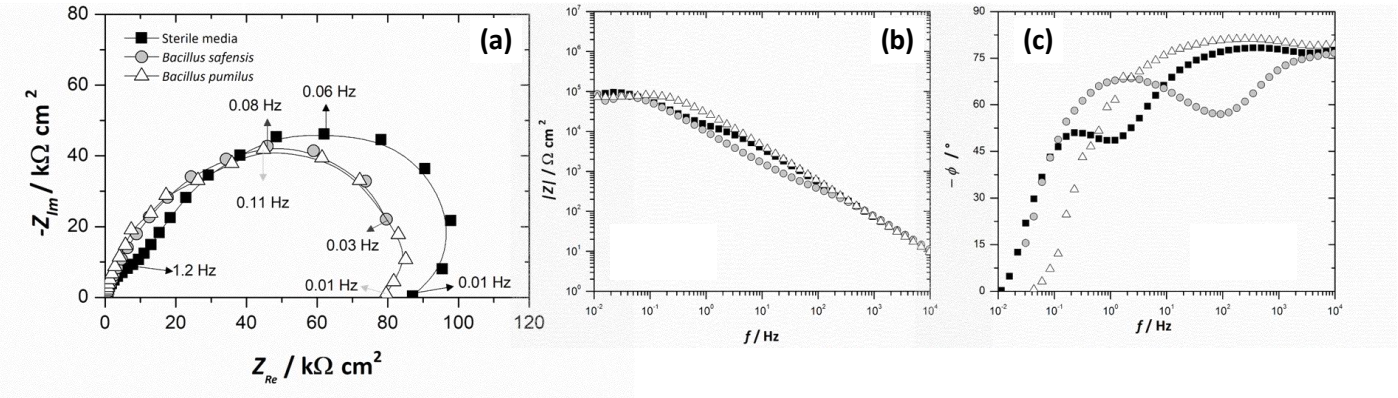

Figure 4 Impedance response collected at E_{OC} of AA2024-T3 after 1 day of exposure. (a) Nyquist, (b) Bode-Modulus and (c) Bode-Phase diagrams.

Table 1 EIS at E_{OC} parameters obtained by graphical method.

Medium	Time	HF				LF	
		Re	C_∞ x10^{-6}	α_{HF}	Q_{HF} x10^{-6}	R_{ct} x10^{3}	C_{dl} x10^{-6}
	(day)	($\Omega \cdot cm^2$)	($F \cdot cm^{-2}$)	(-)	($\Omega^{-1} \cdot s^{\alpha} \cdot cm^{-2}$)	($\Omega \cdot cm^2$)	F cm^{-2}
Sterile	1	70.5	1.5	0.87	7.0	90.92	23.7
	8	60.6	1.2	0.82	9.4	23.62	24.9
	12	70.1	1.5	0.71	21.3	5.51	33.2
B. safensis	1	55.2	1.4	0.85	7.9	86.37	20.6
	8	55.2	1.1	0.82	9.4	29.00	22.9
	12	53.0	0.7	0.71	20.8	9.37	-
B. pumilus	1	57.8	1.6	0.90	5.3	72.04	-
	8	3.7	1.5	0.95	14.6	16.31	41.1
	12	66.9	1.2	0.75	26.6	19.50	17.0

Table 2 shows that the resistance of the electrolyte (Re) exhibited values slightly higher in sterile solution than the inoculated media. The variation has been reported previously [30],[31],[32], which could be related to the bacterial metabolism and/or survival of them [31][33], that would affect the conductivity of the solution directly due to cell lyses [34]. On the other hand, the CPE parameters α_{HF} and Q_{HF} varied among the evaluated systems and as a function of time [35]. Furthermore, the α values showed a decrease as a function of time, which could be related to a deterioration increase of the surface with the exposure time. Q_{HF} parameters which were related to the oxide layer, vary as a function of time, but not among the evaluated systems. Therefore, by EIS to E_{OC}, an influence of bacteria in the oxide layer is not appreciable. However, C_{dl} of the electric double layer (EDL), was impacted by the bacteria presence, showing a rise in the value compared with the sterile medium. Indeed, Kim *et al*. [36] studied the influence of bacteria on the double layer capacitance by EIS, ensure that the technique could provide a monitoring parameter of the bacterial adhesion and biofilm

maturation. The rise of C_{dl} could be related to the increase of bacterial metabolism and its electrode area contribution [36].

On other hand thickness oxide can be estimated through C_{∞} values reported in Table 2 as described Benoit *et al.* [Electrochimica Acta 201 (2016) 340–347], and considering 11.2 as the permittivity of the oxide film.

A representative equivalent circuit obtained from EIS results is shown in Figure 5 (a) as the inserted diagram. The impedance data were evaluated by DRTools, in order to obtain the Distribution Relaxation Times (DRT) which are shown in Figure 5 (b). The values of different parameters of fitting of EIS data are shown in Table S2 in supplementary material.

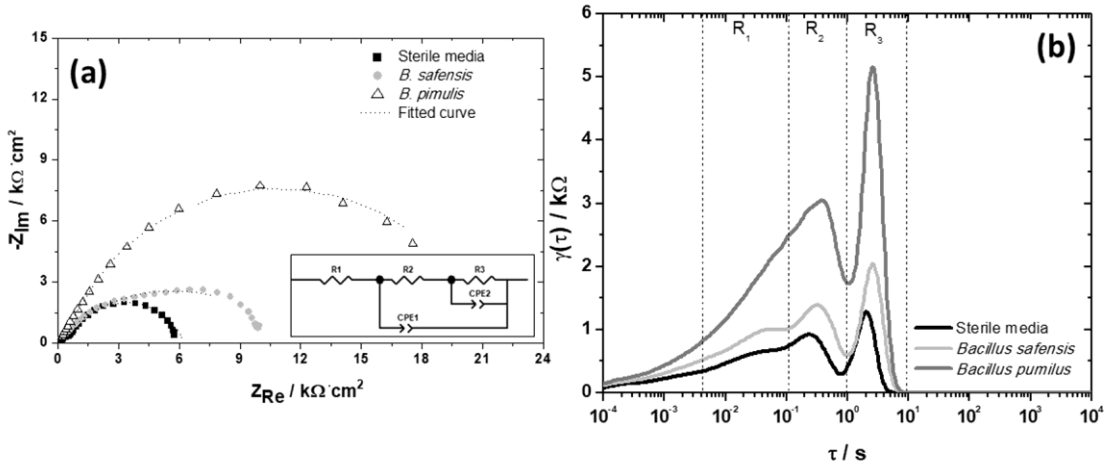

Figure 5 Diagrams obtained of (a) Nyquist plots and fitted curves at 12 days of AA2024 exposed to different conditions with the equivalent circuit (insert), and (b) distribution relaxation times (DRT) from impedance spectroscopy (EIS) data.

As was observed the adjusted parameters after 12 days of exposure, the values achieved were similar that was estimated by the graphical method, making the equivalent circuit a valid representation proposal.

3.5 Electrochemical Impedance Spectroscopy at cathodic potential

From the LSV curves after 1 day of exposure (see Figure 2), a variation in current densities is observed in the cathodic overpotential zone due to the influence of bacteria. The inoculated systems have cathodic currents higher by approximately one order of magnitude more than the sterile medium. In order to understand the possible influence of bacteria, EIS at E vs. SCE= E_{OC} -50 mV was carried out after 1 day of exposure.

Observing the results of the cathodic impedance of the Nyquist diagram in Figure 6 (a), a capacitive loop is visible in the entire frequency range for all systems, indicating the presence of a time constant, with respect to the EIS in E_{OC} where two constants are presented. It can also be observed that the inoculated systems have a lower impedance in an order of magnitude with respect to the sterile system, as well as in the Bode module (see Table 3), revealing a decrease in the corrosion resistance of the alloy in the presence of bacteria. This behavior may be related to the increased current caused by exposure to bacteria shown in the cathodic zone of the LSV curve.

Both responses could indicate that *B. safensis* and *B. pumilus* bacteria are involved in the cathodic reactions that occur on the surface of the alloy.

As presented in Table 3, the LF module ($|Z|_{LF}$), in the sterile system exhibits values around $3x10^6$ Ω·cm^2, while bacteria *B. safensis* and *B. pumilus* smaller values were obtained, $7x10^5$ Ω·cm^2 and $3x10^5$ Ω·cm^2, respectively. The IZI_{LF} value represents the transfer charge resistance related to the cathodic reaction, the IZI_{LF} values of AA2024-T3 decrease in the presence of both bacteria, indicating an influence on this half reaction. On the

other hand, in Tables 2 it was observed that the Re values are similar, that is, there is no considerable variation in the electrolytic medium. The C_∞ at cathodic potential is one order of magnitude less than that of E_{OC}, while the values of α are higher. The parameter Q_{eff} at the cathodic potential has a decrease of one order of magnitude and a modulus of impedance greater by one order of magnitude with respect to EIS to E_{OC}. This observation is due to the polarization allows to see only the cathodic reaction of oxygen reduction reaction, related to a more active and heterogeneous surface, a consequence of the slight polarization applied, but which amplifies the cathodic effect that bacteria induce in the AA2024 alloy-T3.

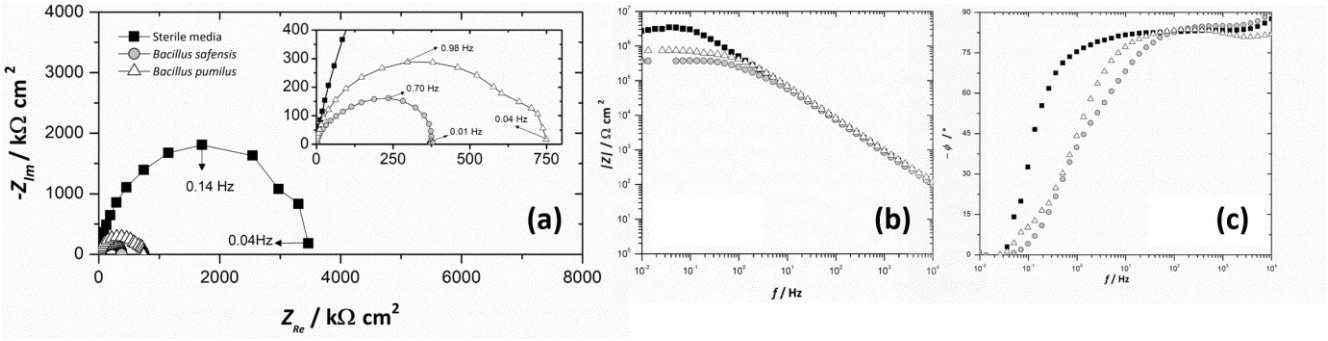

Figure 6 EIS diagrams at cathodic potential of AA2024-T3 (a) Nyquist, (b) Bode-Modulus and (c) Bode-Phase after 1 day exposure.

Table 3. EIS cathodic parameters obtained by graphical method

Medium	Re	C_∞	α	$Q_{eff\ 1315Hz}$	$\|Z\|_{LF}$	C_{dl}
	($\Omega \cdot cm^2$)	($\mu F \cdot cm^{-2}$)	(-)	($\mu\Omega^{-1} \cdot s^{\alpha} \cdot cm^{-2}$)	($k\Omega \cdot cm^2$)	μ
Sterile	62.96	0.15	0.92	0.35	2878.54	0.46
B. safensis	73.96	0.16	0.94	0.33	368.87	0.41
B. pumilus	80.36	0.13	0.93	0.31	739.95	0.40

3.6 Surface characterization

This project has allowed collaboration with the MRDC (Military Research and Development Centre). Napachat PhD. has participated in the preparation of this report with the analysis of electronic images.

In order to clarify the contribution of the bacteria *B. safensis* and *B. pumilus* in the corrosion process at the specific conditions studied, the oxide film was analyzed by top and cross-sections images obtained by SEM-EDX after 12 days of exposure in sterile medium and in presence of B. safensis and B. pumilus media.

It is important to mention that it was not possible to identify the morphology of the bacteria because they were not fixed to the metallic surface, therefore they are not visible in the SEM images. Similarly, the structure of the oxide film was also not identified because of the thickness of the layer is thin, between 6.7 – 14.4 nm.

On the other hand, in general, all the samples showed as the main components of the oxide layer, aluminium and oxygen and consequently it is only included the EDS analysis of the sterile sample (see Figure 7 (a) for details). Likewise, all the samples present polishing defects, which are related to the preparation procedure described in Section 1.1. Regarding Figure 7 (b) and (c), the presence of the bacteria *B. safensis* and *B. pumilus* do not show significant changes on the surfaces, however, considering the effects of the bacteria B. safensis in the electrochemical behavior of AA2024-T3, it was decided to analyze the aluminium surface by cross-section (see Figure 8 for details), revealing the formation of a oxide layer with presence of multiple cracks and a clear localized deterioration; which is consistent with the LSV analysis of an unstable and brittle aluminium oxide film after 12 days of exposure.

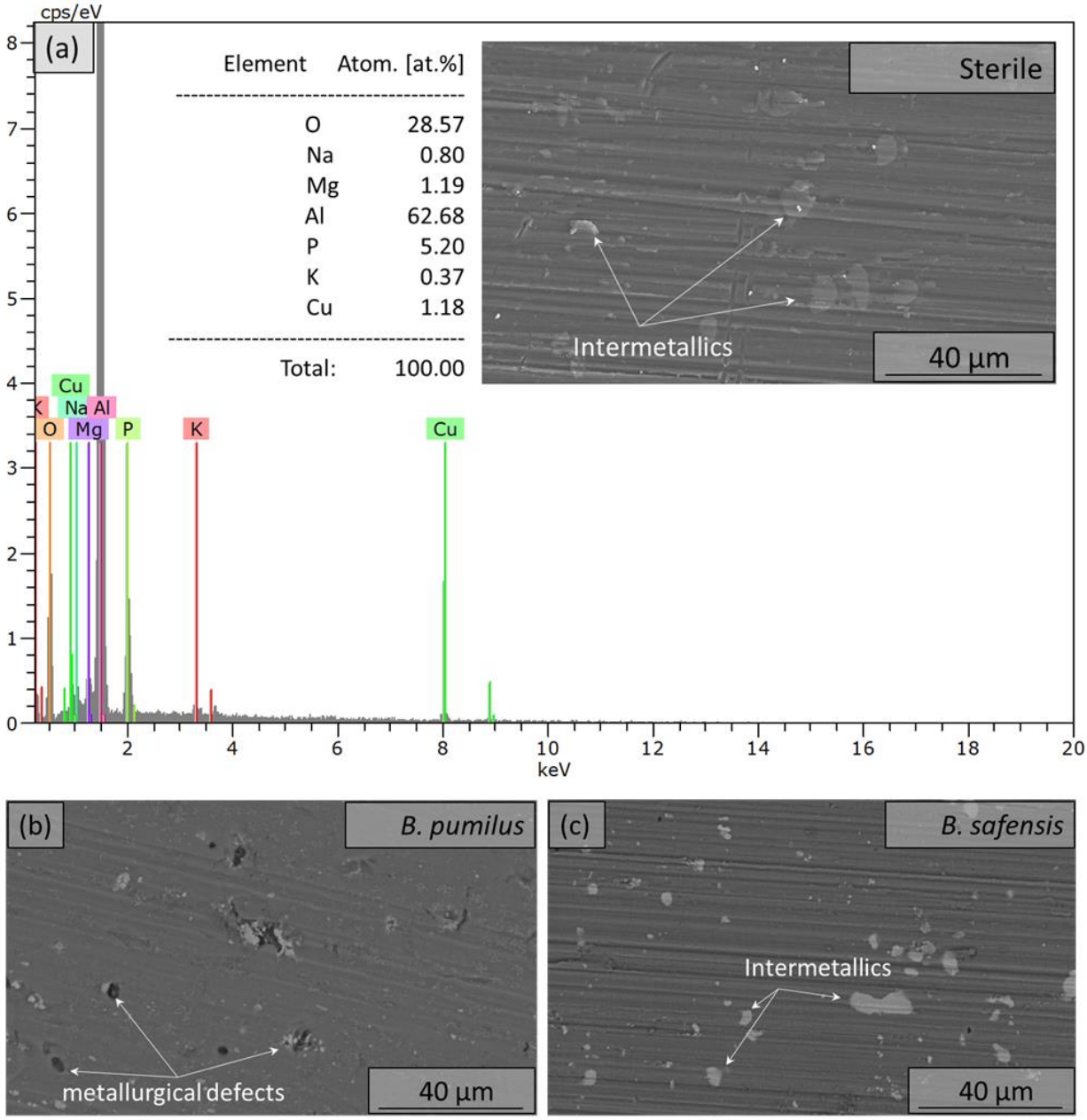

Figure 7 SEM images of AA2024-T3 after 12 days of exposure to SSM media at 30°C ± 2 °C in: (a) sterile, (c) *B. safensis* and (d) *B. pumilus* medium.

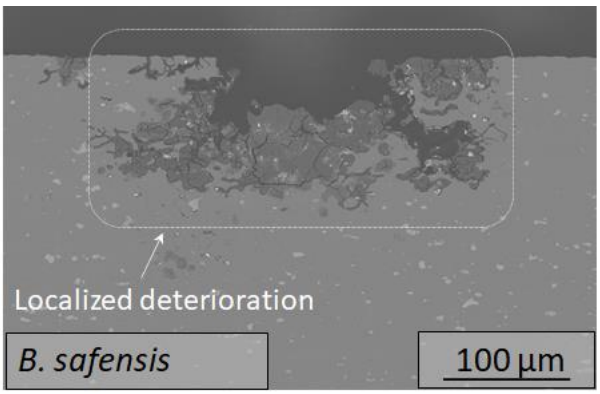

Figure 8 Cross-section image of AA2024-T3 after 12 days of exposure to SSM media at 30°C ± 2 °C with *B. safensis.*

4 CONCLUSIONS

(a) From the corrosion products founded on the aircraft in Thailand, two bacterial species related to the bacillus gene were identified as *B. Pumilus* and *B. safensis*. The influence of these bacteria on the corrosion of AA2024-T3 were evaluated by electrochemical techniques. The LSV plot showed that AA2024-T3 decreased the i_a values after 1 day of exposure to bacteria in comparison with the sterile medium. However, the i_c increase in presence of bacteria, indicating an influence on the cathodic reaction of redox process. On the other hand, the LSV results showed an increase of current density after plateau zone in anodic branch, this behavior could be related to a local corrosion promoted by bacteria. EIS was collected at E_{OC} and at cathodic overpotential, showing differences about the influence of the bacteria on the surface. Regarding to EIS at E_{OC}, *B. pumilus* and *B. safensis* bacteria modified the impedance parameters related to the electric double layer and the electrolyte resistance. In particular, the double-layer capacitance increased in the samples exposed to inoculated media in contrast to the sterile medium, due to an increase in the active area that the metabolic activity of the bacteria would provide. EIS at cathodic overpotential was performed in order to clarify the influence of bacteria on the cathodic reaction after 1 day of exposure. The results threw that the charge transfer resistance drop one magnitude order when AA2024-T3 were exposed to inoculated media compared to the sterile medium.

(b) In respect to SEM images, the top view verifies the presence of a thin alumina oxide layer in both sterile and inoculated samples, without significant differences in the appearances and thickness between them. About cross-section, the sample inoculated confirms localized corrosion which can be associated to the bacterial metabolic activity.

(c) Finally, the evaluation of the influence corrosion behavior of bacteria on AA2024-T3, let us goal was achieved planned.

In relation to these results, a scientific article is in progress to be published. This publish is joint with MRDC of Thailand. This fact has been very important for CIDCA because give us an opportunity of future collaboration.

5 Student formation

Thesis of ungraduated Aeronautical Engineering student

a) Evaluation of electrochemical behavior of aluminium 2024 exposure to organic acid associated to biocorrosion. Enzo Vassallucci.
b) Evaluation of electrochemical behavior of 2024 aluminium alloy exposure to bacteria collected collected of Thailand Military aircraft. Sebastian Gutierrez.

6 *Scientific production*

Congress 2018

Electrochemical behavior of an aluminium alloy surface modified with palmitic acid under biotic and abiotic conditions. Nelson Vejar, Daniela Godoy, Roberto Solis, Claudia Alvarado, Lisa Muñoz, Mamie Sancy y Maritza Páez. 11th International Symposia on Electrochemical Impedance Spectroscopy in Lège-Cap-Ferret, France

Articles

Sol–gel coatings doped with encapsulated silver nanoparticles: inhibition of biocorrosion on 2024-T3 aluminum alloy promoted by *Pseudomonas aeruginosa* E.A. González, N. Leiva, **N. Vejar,** M. Sancy, M. Gulppi, M.I. Azócar, G. Gomez, L. Tamayo, X. Zhou, G.E. Thompson, M.A. Páez. Journal of Materials Research and Technology
Volume 8, Issue 2, April 2019, Pages 1809-1818

Gulppi, M., Munoz, L., **Vejar, N.,** Blamey, J. M., Gonzalez, E., Azócar, M., & Paez, M. (2019). Electrochemical dynamic sensing of hydrogen peroxide in the presence of microorganisms. Electrochimica Acta, 305, 416-422

6. Relation MRDC-CIDCA

The metal samples exposed to bacteria were sent to Thailand for analysis by SEM (June2019). Thanks to this scholarship, the researcher Napachat PhD., from MRDC of Thailand, contributed to this report. In August 2019, at a scientific conference (CRIMPSON VIPER), CIDCA visited the Napachat PhD. Corrosion Laboratory, in order to jointly analyze the results obtained by SEM.

REFERENCES

[1] A. Hughes, T.H. Muster, A. Boag, A.M. Glenn, C. Luo, X. Zhou, G.E. Thompson, D. McCulloch, Co-operative corrosion phenomena, Corros. Sci. 52 (2010) 665–668. doi:10.1016/j.corsci.2009.10.021.

[2] R.G. Buchheit, Local Dissolution Phenomena Associated with S Phase (Al[sub 2]CuMg) Particles in Aluminum Alloy 2024-T3, J. Electrochem. Soc. 144 (1997) 2621. doi:10.1149/1.1837874.

[3] B.J. Little, J.S. Lee, Microbiologically Influenced Corrosion, 2007. doi:10.1002/047011245X.

[4] C.J. McNamara, T.D. Perry, R. Leard, K. Bearce, J. Dante, R. Mitchell, Corrosion of aluminum alloy 2024 by microorganisms isolated from aircraft fuel tanks, Biofouling. 21 (2005) 257–265. doi:10.1080/08927010500389921.

[5] M.E. Rauch, H.W. Graef, S.M. Rozenzhak, S.E. Jones, C. a Bleckmann, R.L. Kruger, R.R. Naik, M.O. Stone, Characterization of microbial contamination in United States Air Force aviation fuel tanks., J. Ind. Microbiol. Biotechnol. 33 (2006) 29–36. doi:10.1007/s10295-005-0023-x.

[6] A.J.M. Stams, C.M. Plugge, Electron transfer in syntrophic communities of anaerobic bacteria and archaea, Nat. Rev. Microbiol. 7 (2009) 568–577. doi:10.1038/nrmicro2166.

[7] S. Sun, Q. Zheng, D. Li, J. Wen, Long-term atmospheric corrosion behaviour of aluminium alloys 2024 and 7075 in urban, coastal and industrial environments, Corros. Sci. 51 (2009) 719–727. doi:10.1016/j.corsci.2009.01.016.

[8] E.L. Iannotti, D. Kafkewitz, M.J. Wolin, M.P. Bryant, Glucose fermentation products of Ruminococcus

albus grown in continuous culture with Vibrio succinogenes: changes caused by interspecies transfer of H2, J. Bacteriol. 114 (1973) 1231–1240.

[9] J. Wu, P. Wang, D. Zhang, S. Chen, Y. Sun, J. Wu, Catalysis of oxygen reduction reaction by an iron-reducing bacterium isolated from marine corrosion product layers, J. Electroanal. Chem. 774 (2016) 83–87. doi:10.1016/j.jelechem.2016.04.053.

[10] C. Alvarado G., M. Sancy, J.M. Blamey, C. Galarce, A. Monsalve, F. Pineda, N. Vejar, M. Páez, Electrochemical characterization of aluminum alloy AA2024 − T3 influenced by bacteria from Antarctica, Electrochim. Acta. 247 (2017) 71–79. doi:10.1016/j.electacta.2017.06.127.

[11] D.A. Jones, P.S. Amy, A thermodynamic interpretation of microbiologically influenced corrosion, Corrosion. 58 (2002) 638–645. doi:10.5006/1.3287692.

[12] J. Hubrecht, J. Vereecken, The Study of the Anodic and Cathodic Corrosion Process of Coated Iron with the Electrochemical Impedance Technique, J. Electrochem. Soc. 132 (1985) 2886–2889. doi:10.1149/1.2113688.

[13] N. D. Vejar, Enhanced Corrosion of 7075 Alloy by the Presence of Bacillus megaterium, Int. J. Electrochem. Sci. 11 (2016) 9723–9733. doi:10.20964/2016.11.33.

[14] M. Sancy, A. Abarzúa, M.I. Azócar, J.M. Blamey, F. Boehmwald, G. Gómez, N. Vejar, M. Páez, Biofilm formation on aluminum alloy 2024 : A laboratory study, 737 (2015) 212–217. doi:10.1016/j.jelechem.2014.08.015.

[15] Q. Wang, G.M. Garrity, J.M. Tiedje, J.R. Cole, Naïve Bayesian classifier for rapid assignment of rRNA sequences into the new bacterial taxonomy, Appl. Environ. Microbiol. 73 (2007) 5261–5267. doi:10.1128/AEM.00062-07.

[16] C. Pillay, J. Lin, Metal corrosion by aerobic bacteria isolated from stimulated corrosion systems: Effects of additional nitrate sources, Int. Biodeterior. Biodegrad. 83 (2013) 158–165. doi:10.1016/j.ibiod.2013.05.013.

[17] Z. Liu, P.H. Chong, A.N. Butt, P. Skeldon, G.E. Thompson, Corrosion mechanism of laser-melted AA 2014 and AA 2024 alloys, Appl. Surf. Sci. 247 (2005) 294–299. doi:10.1016/j.apsusc.2005.01.067.

[18] http://www.ncbi.nlm.nih.gov/BLAST/, (n.d.).

[19] A. Lateef, I.A. Adelere, E.B. Gueguim-Kana, The biology and potential biotechnological applications of Bacillus safensis, Biol. 70 (2015) 411–419. doi:10.1515/biolog-2015-0062.

[20] M. Satomi, M.T. La Duc, K. Venkateswaran, Bacillus safensis sp.nov., isolated from spacecraft and assembly-facility surfaces, Int. J. Syst. Evol. Microbiol. 56 (2006) 1735–1740. doi:10.1099/ijs.0.64189-0.

[21] M.T. La Duc, R. Kern, K. Venkateswaran, Microbial monitoring of spacecraft and associated environments, Microb. Ecol. 47 (2004) 150–158. doi:10.1007/s00248-003-1012-0.

[22] M.J. Kempf, F.E.I. Chen, R. Kern, K. Venkateswaran, Resistant Spores of Bacillus pumilus from a Spacecraft, 5 (2005).

[23] K. Venkateswaran, M. Satomi, S. Chung, R. Kern, R. Koukol, C. Basic, D. White, Molecular microbial diversity of a spacecraft assembly facility, Syst. Appl. Microbiol. 24 (2001) 311–320. doi:10.1078/0723-2020-00018.

[24] B. Little, J. Lee, R. Ray, A review of “green” strategies to prevent or mitigate microbiologically influenced corrosion., Biofouling. 23 (2007) 87–97. doi:10.1080/08927010601151782.

[25] S. Sivasankaran, Aluminium Alloys: Recent Trends in Processing, Characterization, Mechanical behavior and Applications, 2017. doi:http://dx.doi.org/10.5772/68032.

[26] K.M. Deen, M. Yousaf, N. Afzal, S. Riaz, S. Naseem, A. Farooq, I.M. Ghauri, Microbiological influenced corrosion attack by Bacillus Megaterium bacteria on Al–Cu alloy , Mater. Technol. 29 (2014) 269–274. doi:10.1179/1753555714y.0000000150.

[27] Y. Shen, Y. Dong, Y. Yang, Q. Li, H. Zhu, W. Zhang, L. Dong, Y. Yin, Study of pitting corrosion inhibition effect on aluminum alloy in seawater by biomineralized film, Bioelectrochemistry. 132 (2020) 107408. doi:10.1016/j.bioelechem.2019.107408.

[28] G. Boisier, N. Portail, N. Pébre, Corrosion inhibition of 2024 aluminium alloy by sodium decanoate, Electrochim. Acta. 55 (2010) 6182–6189. doi:10.1016/j.electacta.2009.10.080.

[29] A.S. Nguyen, N. Causse, M. Musiani, M.E. Orazem, N. Pébère, B. Tribollet, V. Vivier, Determination of water uptake in organic coatings deposited on 2024 aluminium alloy: Comparison between impedance measurements and gravimetry, Prog. Org. Coatings. 112 (2017) 93–100. doi:10.1016/j.porgcoat.2017.07.004.

[30] S. Yu, Y. Lou, D. Zhang, E. Zhou, Z. Li, C. Du, H. Qian, D. Xu, T. Gu, Microbiologically influenced corrosion of 304 stainless steel by nitrate reducing Bacillus cereus in simulated Beijing soil solution, Bioelectrochemistry. 133 (2020). doi:10.1016/j.bioelechem.2020.107477.

[31] F. Laurent, B. Grosgogeat, L. Reclaru, F. Dalard, M. Lissac, Comparison of corrosion behaviour in presence of oral bacteria, Biomaterials. 22 (2001) 2273–2282. doi:10.1016/S0142-9612(00)00416-6.

[32] J. Atalah, L. Blamey, H. Köhler, H.M. Alfaro-Valdés, C. Galarce, C. Alvarado, M. Sancy, M. Páez, J.M. Blamey, Study of an Antarctic thermophilic consortium and its influence on the electrochemical behavior of aluminum alloy 7075-T6, Bioelectrochemistry. 133 (2020). doi:10.1016/j.bioelechem.2019.107450.

[33] I. Part, B.Y.C. Shearee, STUDIES ON THE ACTION OF ELECTROLYTES ON BACTERIA . Action of Electrolytes on Bacteria, (2020) 337–360.

[34] M. Grossi, B. Riccò, Electrical impedance spectroscopy (EIS) for biological analysis and food characterization: A review, J. Sensors Sens. Syst. 6 (2017) 303–325. doi:10.5194/jsss-6-303-2017.

[35] M.E. Orazem, I. Frateur, B. Tribollet, V. Vivier, S. Marcelin, N. Pébère, A.L. Bunge, E.A. White, D.P. Riemer, M. Musiani, Dielectric Properties of Materials Showing Constant-Phase-Element (CPE) Impedance Response, J. Electrochem. Soc. 160 (2013) C215–C225. doi:10.1149/2.033306jes.

[36] T. Kim, J. Kang, J.H. Lee, J. Yoon, Influence of attached bacteria and biofilm on double-layer capacitance during biofilm monitoring by electrochemical impedance spectroscopy, Water Res. 45 (2011) 4615–4622. doi:10.1016/j.watres.2011.06.010.